DESIGN OF NOVEL LOWER BODY EXOSKELETON

Nathan Folta

Department of Mechanical Engineering, Virginia Tech

Advisor: Dr. Alan Asbeck

Abstract

This paper presents the novel design of a lower-body exoskeleton to aid human walking, stability, and control; designed to support up to 80% user bodyweight with ground reaction force for the 50th percentile male weight equal to 667 N (150 lbf) and height of 175.3 cm (5'9") at maximum and 165 cm (5'5") at minimum. It will allow users to walk comfortably up to 2 m/s (4.5 mph) and perform minimal squatting (60-90 deg knee flexion) in partial sitting and resting positions depending on user height. Powered by a single sprocket-chain driven prismatic leg actuator on each leg, the device applies force from the ground to the wearer's center of mass to simulate the user feeling up to 80% lighter or, in reverse function, 80% heavier. Targeted application includes simulation of gravity-like conditions for pre-mission training, enhanced locomotion or resistance exercise in microgravity environments during-mission, and support for transitions back to earth in post-mission recovery. The mechanical design is optimized for simplicity, ease of assembly, low cost, and lightweight. A key feature of the exoskeleton is the ability for the hip to freely rotate, allowing the wearer to choose their footstep locations without interference from the frame to provide a natural walking experience.

Introduction

Lower body exoskeletons are wearable devices that are designed to support, augment, or replace the function of the lower limbs. They have numerous applications including medical rehabilitation, industrial aid and production, injury prevention, military training and mission, and space exploration.

There are a variety of lower body exoskeletons for repetitive lower limb movements, some with upper body structure to allow attachment of objects to the back or chest. Of these, the exoskeletons most relevant to our work are those that are under-actuated, i.e. have fewer powered Degrees Of Freedom (DOF) than joints they are assisting.

An exoskeleton called OLAD was designed to assist soldiers with loaded walking [3], using a single actuator extending from the backpack to the heel of the foot. It weighs less than 7 kg, requires 30 to 40 watts of electricity during walking, and can carry 36 kg. Similarly, Exobuddy, a non-anthropomorphic exoskeleton, assists the joints and muscle-tendon complex by transferring the carried load from a backpack to the ground via a parallel mechanism, which weighed 21.8 kg [9]. During experimental walking with 40 kg backpack, 30% of the load was transferred to the ground.

A wearable lower-limb exoskeleton was developed to assist with repetitive lower-limb activity and minimized muscular activation by 36% during lifting a box of 4.3 kg (9.48 lbs) from the ground, holding it for a while, and placing it back on the floor [8]. The exoskeleton consists of one active and one passive DOF at the hip joint, one active and one passive DOF at the knee joint, and two passive DOFs at the ankle joint. Bi-directional brushless DC motors operate the active DOFs to enable sagittal motions. [6] developed an electrically actuated lower extremity exoskeleton for walking assistance. The knee joint actively actuated, and the actuation system contained a DC motor, a gear transmission structure, and a ballscrew. The other joints are linked by elastic parts and passively actuated. [4] developed a similar exoskeleton for walking while load carrying PALExo, a Parallel Actuated Lower Limb Exoskeleton for high-load carrying with two linear actuators per leg extending from the waist to the foot [10]. The parallel structure is suitable for heavy load bearing while allowing for comfort with little attachment to the legs at the knee joint, avoiding the misalignment of parallel structure exoskeletons. Each of these examples proposes a solution to the problem of heavy lifting, however they all use one motor per joint resulting in reasonably high weight and complexity. This presents opportunity for a novel underactuated system with a mechanical design optimized for simplicity, ease of assembly, low cost, and lightweight.

While there are a variety of applications for lower body exoskeletons, one of particular interest is training, exercise, and post-mission rehabilitation surrounding space activity. The exoskeleton can simulate gravity-like conditions for pre-mission training, enhance locomotion in microgravity environments during-mission, provide resistance walking exercise in microgravity conditions, and support transitions back to earth in post-mission recovery. Astronauts in space experience a range of physiological changes due to the lack of gravity, such as up to 30% muscle atrophy [2], 2.5% average bone density loss, and significant cardiovascular deconditioning [5], requiring rehabilitation for proper recovery [7]. Devices built to operate under microgravity conditions such as the Advanced Resistive Exercise Device [1] effectively provide training but are limited to localized spaces and typically are bulky and heavy. An exoskeleton prototype such as the one we are presenting present could help mitigate these effects in space by providing resistance during exercise, aiding maintenance of muscle and bone mass and cardiovascular fitness for long periods of time during other activities. Additionally, the sudden transition from microgravity to earth's gravity can be jarring and can cause physical discomfort and impairments. Our prototype could be applied to help astronauts transition back to Earth's gravity by gradually increasing the amount of weight bearing and providing support and assistance during rehabilitation exercises. Overall, opportunities for the application of lower body exoskeleton are endless to aid in all stages of space travel by altering the effects of gravity and enhancing locomotion.

Overview

The purpose of this research project is to design and build a novel lower body exoskeleton to aid human walking, stability, and control in a variety of applications. The assistive device will be designed to support up to 80% bodyweight (BW) ground reaction force for the 50th percentile male equal to 667 N (150 lb-f) and height of 175.3 cm (5'9") at maximum and 165 cm (5'5') at minimum. It will allow all users to walk comfortably and unrestrained up to 2 m/s (4.5 mph), and minimal squatting (60 deg knee flexion) and resting positions, while not designed to allow for comfortable sitting.

The device is powered by a single prismatic leg actuator that will apply force from the ground to the wearer's center of mass. A key feature of the exoskeleton is the ability for the hip to freely rotate, allowing the wearer to choose their footstep locations without interference from the exoskeleton, allowing for a natural walking experience.

Figure 1 shows an overview of the design. Normally during walking, the joints in the leg (hip, knee, ankle) work together to create a net Ground Reaction Force (GRF) that passes approximately through the body's center of mass, which is located near the waist in the center of

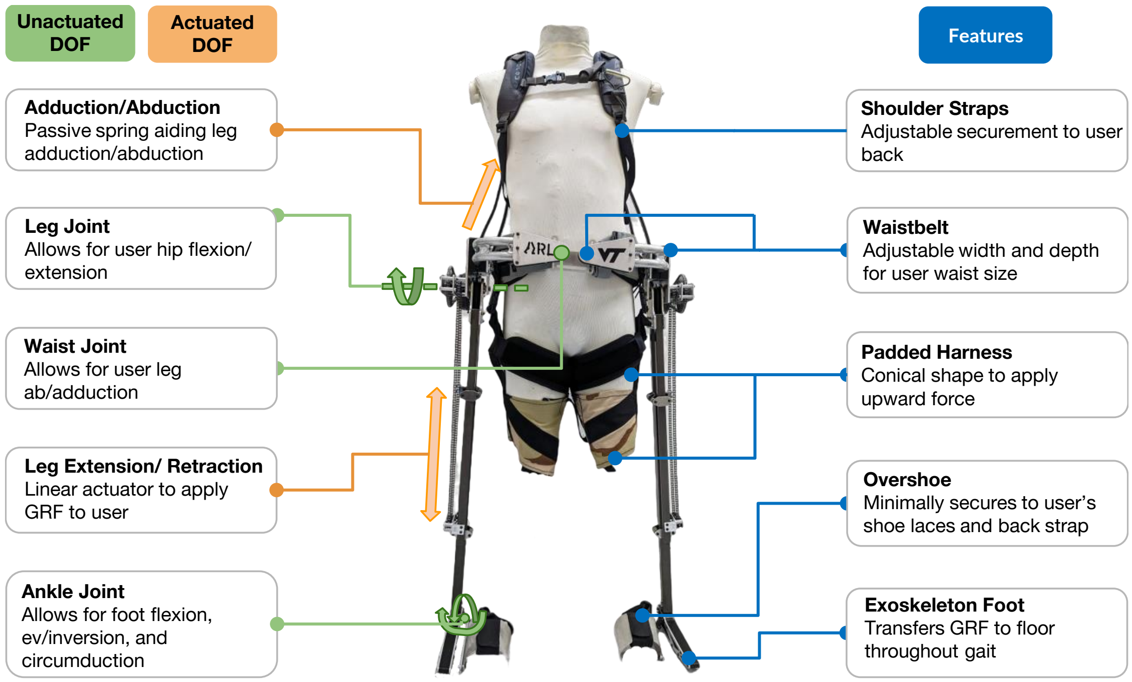

Figure 1: Exoskeleton design system overview depicting various features and actuated and unactuated DOF.

the body. Our objective is to generate a similar force from the ground through the body's center of mass, but with a single actuator, shown in Figure 2. This is accomplished by a linear (prismatic) actuator running down the side of the body, with a mechanical linkage transferring the force to the center of the body. The hip is unactuated, allowing the wearer full control over the location of each footstep.

The exoskeleton aid locomotion by extending during the Stance phase of walking, creating a force just like the foot; then during the Swing phase, retracting to clear the floor allowing the wearer to move freely. The overshoe is attached on a linkage arm with three DOF allowing for free flexion, eversion and inversion, and circumduction the foot/leg.

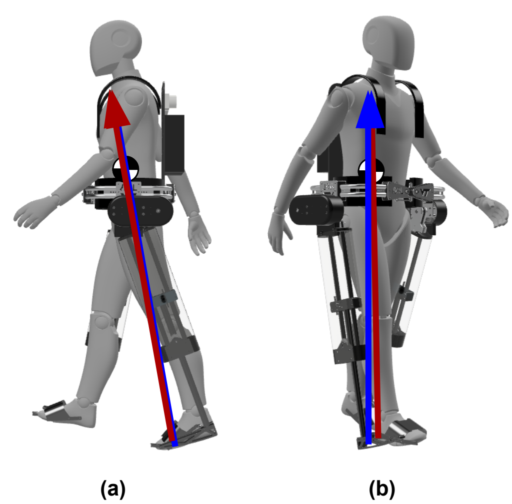

Figure 2: Fully body CAD design illustration of the GRF acting on the user (red arrow), and acting through exoskeleton (blue arrow) in (a) side view left foot, and (b) isometric view right foot with the exoskeleton .

Mechanical and System Design

The exoskeleton is made up of six main assemblies: the overshoe, linear frame, motor, waist belt, backplate, and user interface. Each system was designed to meet the aforementioned specifications and four objectives:

simplicity, ease of assembly, low cost, and lightweight, as well as mechanically maintaining a factor of safety of at least 2.5. Each assembly progressed through an iterative design process where both qualitative and quantitative decisions were made to meet the objectives and appropriate specifications for the desired use case scenario. The following sections highlight the design process for each of the main assemblies.

Overshoe Foot Assembly The purpose of the overshoe is to secure the exoskeleton foot to the user's foot, while effectively allowing the GRF to be transferred through the frame. Unrestricted walking range of motion, ease of adjustability, and infrastructure for sensing gait cycle were the primary design objectives. Several designs and attachment methods were proposed, reviewed, and down-selected to one final design consisting of a thin 1.2 mm (3/64 in) aluminum U-shaped overshoe bent to the user's foot profile and secured on the laces and heel with straps and velcro. This allows for easy securement on any close toed shoe with laces.

Waist-belt Assembly The objective of the waist-belt assembly is to transfer the BW support from the exoskeleton legs to the user's center of mass between the hips while permitting a range of motion for walking and squatting. To achieve an optimal system, numerous design and prototype iterations were proposed, tested, and down-selected. Among these, a four-bar parallel plate design with a pivoting attachment plate having a center of rotation at the user's Center Of Mass (COM) was initially considered but ultimately replaced with a modular system with adjustable sizes. This modular assembly, comprised of dual tube filet weld-supported aluminum, incorporates four adjustable pieces for accommodating users of varying sizes, joined with aluminum supported 3D printed bolted assembly.

In order to support a user while walking comfortably and effectively throughout the gait cy-

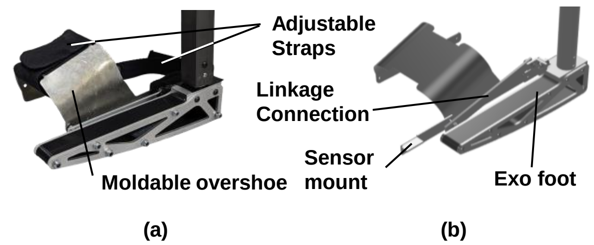

Figure 3: Overshoe features showing (a) prototype and (b) CAD rendering.

cle, the force of the BW support must pass close through the user's standing COM between the hips. To achieve this, the waist-belt must support the user as well as securely fasten to them. Two modular "U" shaped tubes can achieve this. See Figure 2 representing the force location requirement. The sum of the COM acting force must be 80% BW support, at maximum 667 N (150 lbs), with components of the 161.7 N in the X-direction from user COM to the respective hip, 647 N in the Z-direction, and 0 N in the Y while remaining standing with the force acting at an angle of 14 deg from the ground to the center of mass with respect to vertical.

Iterations of the design began with a bent tube base for strength and reduced weight then progressed from single tube to dual tube design to support the high bending force at the hip of 194.1 N-m (143.2 lb-ft). Square and circular tubes were considered, and the circular tubes were found to sustain a higher bending force per weight than square tubes. Various dimensions of circular tubes were then processed MATLAB to evaluate a three variable optimization problem for inner and outer diameter then selected by weight based on available stock tubing from McMasterCarr while meeting a FS requirement of 2.5. This allowed for minimize weight, size, and maximize strength of the system. The critical sections include the top/bottom and the side of the tubes. A 3D mesh plot showing relation between a selected outer diameter, inner diameter, and the calculated Von Mises stress of the tube, demonstrated a plane that represents our max-

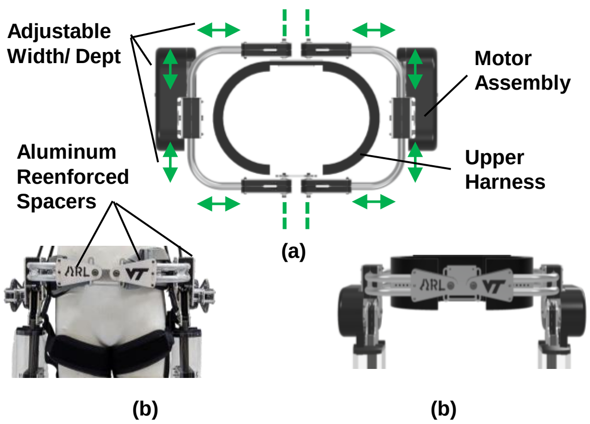

Figure 4: Waistbelt features showing (a), (c) CAD and (b) CAD design.

imum allowable yield strength that maintains the desired FS. Next the intersection between this maximum stress plane and the calculated stress surface demonstrates possible critical dimensions combinations for maintaining the desired FS. Finally a weight optimization was performed to determine which pairing resulted in the lowest weight.

The dementiosn selected were 19.05 mm (0.75 in) OD, 15.75 mm (0.62 in) ID tubes with a 12.7 mm (0.5 in) vertical offset between the two tubes to increase the moment arm to alleviate the bending force. Dual aluminum plates between a custom design plastic spacer was used to clamp onto the tubes with adjustability feature, performing better on double tube than single tubes with lessened shear force acting on bolts as shown when conducting finite element analysis on the assemblies. The spacing between the two tubes also offered efficient mounting for the exoskeleton's passive waistbelt support spring and soft goods (see section below). Figure 4 depicts the final design dual tube assembly and prototype with MIG and TIG fillet welding processes to secure the tubes apart.

Frame Assembly The frame assembly design objective is to effectively support a 80% BW force from the exo foot to the user while keeping from restricting the user's range of motion. In order to accomplish this, the design must be compact and lightweight, in addition to being simplistic for ease of assembly. Different designs were proposed including a parallel four-bar linkage system, and dual and tri-linear retracting square and circular tube design, all with various bearing systems. Each was studied and weight optimization performed to determine the smallest and lightest weight structural material and geometry required to meet a FS of 2.5. Tubular geometry was determined to have the highest bending strength for weight, and similarily to the waist-belt assembly, a three variable optimization was performed to determine the lightest combination of tube width and thickness meeting the given FS. This was also evaluated in MATLAB the same way based on available stock tubing from McMasterCarr.

The net bending forces acting at the upper and lower bearings were 651.5 N (146.46 lbf) and 607 N (136.50 lbf) respectively. The bearing sustains a force of 111.2 N (25 lbf) acting on the chain attached to the upper assembly. The optimized circular tube geometry was 19.05 mm (¾ in) outer diameter with a thickness of 2.1 mm (0.083 in) for the two outer tubes, and 25.4 mm (1 in) outer diameter with thickness of 2.431 mm (0.095 in) for the inner tube. The square geometries version had the same outer dimension, but thickness of 1.58 mm (0.062 in) as the square geometry is stronger in bending.

The linear four bar system, while having advantage with the added degree of motion articulation at the knee, required an impractical amount of torque (upwards of 300 N-m) demanding stronger and heavier structural tubing that made it unfeasible for weight and bulkiness. The dual and tri-linear retracting tube designs required much less torque (6.6 N-m), and lighter weight tubing as strength peaks with compressive over bending loading. However, the linear actuation minimized the reaction length compared to the four bar, but was still preferred for the other based on weight, size, and actuation power necessities. Various versions of the linear

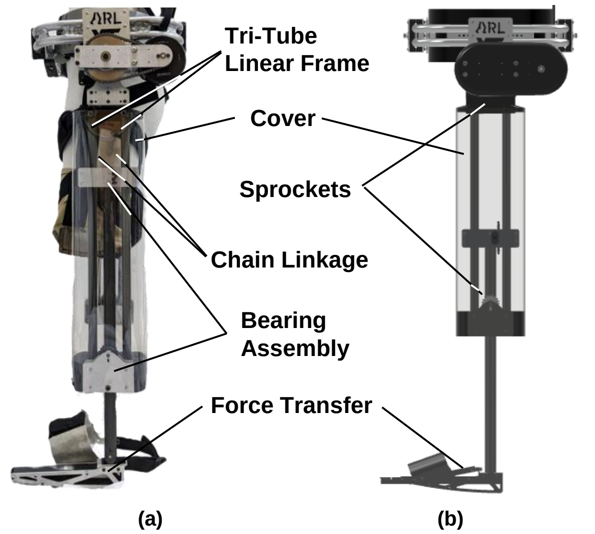

Figure 5: Structural frame design C1 features showing (a) prototype and (b) CAD design.

frame were proposed, including dual and tri-linear tubes, where one or two tubes pointed upwards while the other one or two pointed downwards with two modular bearing assemblies allowing for low friction contact between them. The dual-linear frames introduced large torsional stresses due to the asymmetry which dramatically increased surface contact stresses and friction that compromised the effectiveness of the system, while the 3 tube frames required smaller and lighter weight tubes but supported torsional forces with linear ball bearings in the modular assemblies, as shown in Figure 5).

Contact stress mechanics were then explored to determine resilience of the linear ball bearing systems using MATLAB analysis. Initial calculations showed the aluminum walls surface failed and would sustain grooves from the bearing. This required two possible solutions: anodizing the aluminum tubes for a harder coating, or changing the bearing type. Both were explored and determined to be feasible, and will henceforth be called Configuration 1 (C1) for the circular tri-tube design, and Configuration 2 (C2) for the square tri-tube design (shown in Figure 1). The linear ball bearings performed effectively on anodized aluminum, and a dual roller bearing assembly using square tubing was explored. This design consisted of two bearings, one on each side of each of the three retracting tube frame, where they together supported bending moments across a larger surface area on the square profile.

The chosen bearing for the C1 bearing assembly was a self aligning linear ball bearing (McMaster: 9069T3-4). The critical contact stress was calculated to be 58000 Mpa (8475 ksi), which failed to reach the FS. Anodizing the tubes increase the hardness by a factor great enough to reach the required FS. The bearings for C2 was needle-roller bearings (McMaster: 5905K53) with bushings over a shaft. The critical contact stress was 1590 Mpa (230 ksi) over two bearings, still failing design safety factor, so anodizing was also required to increase the hardness to meet requirements.

The frame is actuated effectively by a prismatic actuator composed of a non-continuous dual fixed sprocket-chain assembly with a link attached to the upper bearing assembly. The two bearings function by retracting and extending governed by the moving no. 25 chain, until hitting the hardstops of maximum lengths at each end.

Motor Assembly The motor assembly is fixed to the waist belt assembly and houses the electric motor, and gear reduction system for transferring torque to the frame assembly for offsetting GRF. Positioning of the motor became an important design criteria to avoid bulky or boxy structures limiting user range of motion, weight distribution, and efficient transfer of power to the frame assembly, while simultaneously required to meeting the minimum factor of safety with the addition of motor weight and induced torque. Several design iterations were performed until developing a compact aluminum assembly that satisfactorily secured the components. The plate thickness was minimized at 3.175 mm (0.125 in) to support torsion forces,

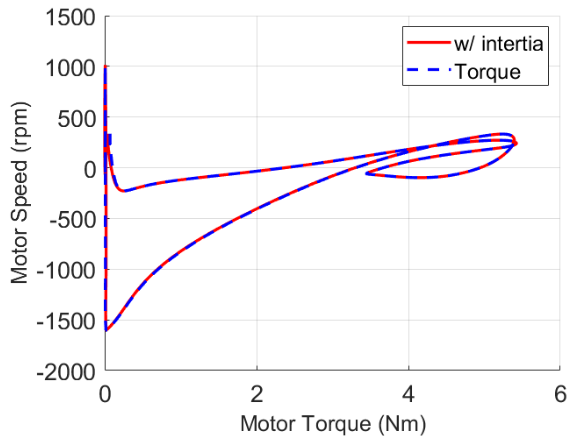

Figure 6: Motor system speed-torque graph with 3:1 GR.

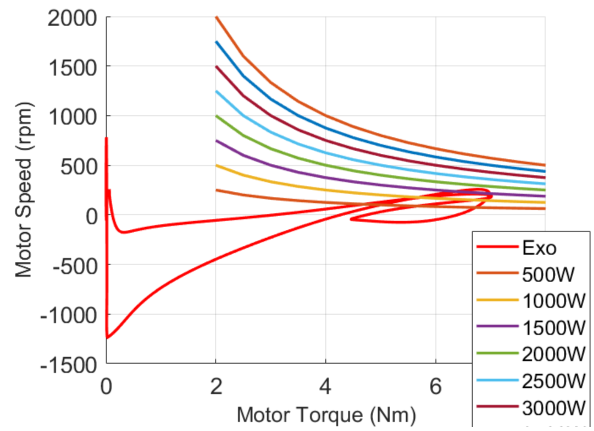

Figure 7: Motor system power requirements.

while sprockets and motors were spaced on a 12 mm (0.47 in) keyed shaft, reaching a factor of safety of 3, higher than required, but warranted for the main power assembly.

Given the two initial frame designs, motor configurations were configured based on the requirements of each. The four bar frame required a lower power motor with low speed but extremely large torque (upwards of 300 N-m at 0.5 rpm) compared to the linear frame requiring a higher powered motor with higher speeds but considerably smaller torque (6.6 N-m and 1305 rpm). Brushless DC motors configurations for the four bar mechanism, initially examining the T-motor AK80-64 motor, required an excessive gear reduction system (6:1 on top of the 64:1 internal reduction to the for lower powered motor), while the linear design was achievable with a lower power motor, the T-motor U13II KV65 with a 3:1 reduction.

With the goal to reduce cost and weight of the exoskeleton system as a whole, the four bar frame design was excessively heavy, and the linear design configuration was selected. The next strategy was to minimize the torque required to drive the exoskeleton while ensuring its optimal performance. The 3:1 reduction ratio was adopted to maintain backdrivability while decreasing standing torque, which, in turn, decreased the battery discharge rate and extended the exoskeleton's lifetime. Calculations were initially carried out for timing belts, but the resulting size of the belts required to withstand the tensile forces on the exoskeleton was deemed unsatisfactory, and the high pitch diameter of pulleys increased required torque. Subsequently, a chain drive was proposed to reduce the pitch diameter at the motor output with little addition in weight. The ANSI #25 roller chain was chosen based on its rated horsepower and tensile strength. A 16 tooth sprocket was selected to both meet the required factor of safety and maintain a smaller 17mm pitch diameter and a larger sprocket of 48 teeth. This reduction decreased the torque requirements of the motor. This can be seen in 6 and plotted against the motor power in 7.

A decision was made based on the plotted torque-speed curve of the U13II motor 6, which showed that the selected reduction ratio was sufficient to limit the current required for the motor during operation. With a reduced torque of 6.6 Nm, the exoskeleton's lifetime was expected to increase.

Backplate and Exo Support Assemblies

The backplate will be secured to the user's body with backpack-like straps and house the electronics and power systems in addition to

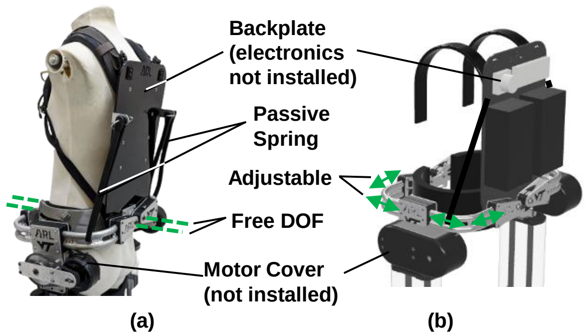

Figure 8: Backplate features showing (a), (c) CAD and (b) CAD design.

the gravity compensation system. Made from 4.8 mm (3/16 in) thick acrylic plate reinforced with aluminum, the backplate is secured to the outside of the waist belt held to the body by shoulder straps like a backpack. The gravity compensation system consists of two elastic tubing fixed at the backplate aluminum support and the waist belt at a distance with the given spring constant (300 N-m) required to suspend the weight of one leg (10.4 lbs, 4.7 kg) and allow for free abduction/adduction of the leg.

Human Interface Harness Assemblies The transfer of full GRF to the user without causing discomfort, counterbalancing, or impeding the active range of motion poses a significant challenge for exoskeleton design. To overcome this issue, a human interfaced harness system was carefully designed and tested in several design iterations with 80% BW support, until a final prototype was manufactured using a combination of parts from a utility harness, straps, cloth, buckles, and velcro.

The design features a two-stage adjustable system that allows for even and comfortable force distribution through a combination of lower and upper thigh straps that are connected to the waist belt. The waist belt serves to center the mechanical assembly on the user and channel the upward BW support force generated. In particular, a conical shape wide cloth strap for the lower thigh was found to be optimal for applying distributed force when pulled upward by the exoskeleton.

Electronics and Controls

In the course of developing the exoskeleton frame, the electronic and control system was concurrently in progress using a previous prototype as a reference point, however, substantial redesign was necessary to meet the specifications of the current project. Consequently, the electronics underwent modifications on the completed exoskeleton, and data collection was initiated for a preliminary version of the control system. The sensors that were implemented in a previous exoskeleton prototype bear resemblance to those that will be integrated into the presented exoskeleton design.

Gait Detection System One IMU sensor was integrated into the overshoe for gait detection on each foot. The IMU sensor employed was the BNO055 9 DOF Absolute Orientation IMU Fusion Breakout Board (Adafruit PN: 2472), positioned at the knee of the exoskeleton to detect hip flexion/extension angle and angular velocity. This sensor, in conjunction with a 10 cm long, 10 kOhm linear potentiometers (Digi-key PN: 987-1407-ND) integrated into the actuator rod, were used to detect the six gait phases: flat foot, heel-off, toe-off, back swing, front swing, and heel strike.

IMU and linear potentiometer were connected to a microcontroller (Adafruit ESP32 feather) to process the data. The microcontroller collected the data and converted them into low and high bytes before sending them to a CAN transceiver chip, MCP2551 (Digi-key PN: MCP2551-I/P-ND). To distinguish between the two legs, the CAN transceiver chip had different IDs, with the right leg having ID 0x01 and the left leg having ID 0x02. The entire electronics system was constructed and implemented for accurate gait detection.

Another microcontroller of the same type was placed on the back of the exoskeleton, connected to a motor controller and a CAN transceiver.

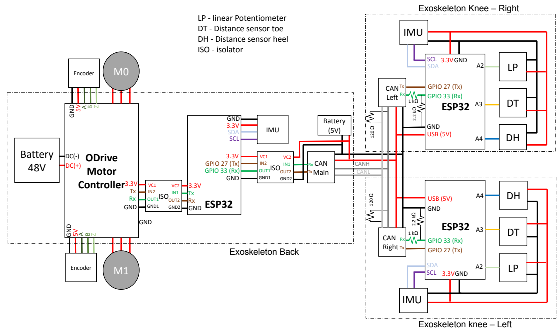

Figure 9: Circuit diagram.

The CAN transceiver received the data sent by the other two transceivers on the legs. Data is transferred between the CAN transceiver through CANH and CANL lines. The microcontroller is connected to the Odrive Motor controller through UART communication. The Motor controller would be connected to two 24 V batteries in series, making a 48 V total, which powers the Odrive and the motors. The purpose of the microcontroller: 1) maintain communication with the Odrive motor controller, and 2) receive data from the two other microcontrollers and detect gait. Currently, the microcontroller can receive data and detect gait. To avoid the high-power Odrive from causing EMI emission in the CAN transmission line, ferrite rings (Digikey PN: 399-10854-ND) were placed around the motor wire. Two isolators (Digi-key PN: 296-50304-ND), one between the ESP32 and CAN transceiver and one between the ESP32 and odrive, were also used for noise reduction. The overall circuit diagram is shown in the figure below.

Discussion

The key objectives and specifications of the design were addressed as follows. As an underactuated system made from parts from three primary suppliers, the design remained simplistic and easy to assembly. The cost of each exoskeleton configuration was $3500, under the targeted $4000. The design remained simplistic and easy to assemble with mechanical parts available from three main suppliers, and with the addition of outsourced laser metal cutting provider, able to be assembled with simple hardware installation, chain and sprocket assembly, and a few specialty parts and functions such as custom harness soft good sewing, 3D PLA extrusion plastic printing, and rivet nut installation. The mechanical structure and motor weighs about 20 lbs (9kg), remaining lightweight while negligible to the user as the frame supports its own weight. All mechanical components maintained a factor of safety of at least 2.5 to effectively support 80% BW of the 50th percentile male.

The presented exoskeleton has the potential to mimic microgravity conditions for pre-mission training, improve mobility in microgravity environments during missions, facilitate resistance walking exercises in microgravity conditions, and assist in post-mission recovery by mitigating the adverse effects of space travel on the human body. First, the exoskeleton could supply a percentage of BW support up to 80% applied to the user's COM, mimicking the weightless walking experienced in space. During mission operations, the exoskeleton function could be applied in reverse and compress the user's lower body into the floor to provide mobile weight resistance for exercise and training during any activity to help maintain muscle, bone mass, and cardiovascular fitness for prolonged periods. Furthermore, physical discomfort and impairments during return to Earth's gravity from microgravity could be addressed with the exoskeleton gradually increasing the weight bearing and supporting them during rehabilitation exercises.

Future Work

As described, the comprehensive scope of this project includes the integration of sensors, electronics, and controls systems to the mechanical and power systems. This would then be verified by testing with walking to understand gait performance, benefit, and proper detection of the gait metrics for further evaluation.

Conclusion

This paper presents a novel design for a lower-body exoskeleton that can support up to 80% of the user's body weight with ground reaction force for the 50th percentile male weight, providing aid for walking, stability, and control. In specific application to training, exercise, and post-mission rehabilitation of space, the design provides the mechanical infrastructure required for 80% BW support to simulate the user feeling up to 80% lighter or heavier for either pre-mission training or resistance exercise in microgravity environments during-mission. While further integration, control, and testing are required for the full extent of verification of this system operation, the mechanical infrastructure is capable and ready for integration.

The proposed novel lower body exoskeleton design and prototype has extensive potential for space travel, contributing to mitigating the effects of gravity on the human body and enhancing locomotion, during all stages of the mission.

References

[1] H. E. Berg and P. A. Tesch. Force and power characteristics of a resistive exercise device for use in space. Acta astronautica, 42(1-8):219–230, 1998.

[2] R. H. Fitts, D. R. Riley, and J. J. Widrick. Functional and structural adaptations of skeletal muscle to microgravity. Journal of Experimental Biology, 204:3201–3208, 2001.

[3] K. W. Hollander, P. Clouse, N. Cahill, A. Boehler, T. G. Sugar, and A. Ayyar. Design of the orthotic load assistance device (OLAD). In 7th Annual Dynamic Walking Conference, pages 172–173, 2012.

[4] W. Kim, H. Lee, D. Lim, C.-S. Han, and J. Han. Development of a lower extremity exoskeleton system for walking assistance while load carrying. In Nature-Inspired Mobile Robotics, pages 35–42. World Scientific, 2013.

[5] A. D. LeBlanc, E. R. Spector, H. J. Evans, and J. D. Sibonga. Skeletal responses to space flight and the bed rest analog: a review. Journal of Musculoskeletal and Neuronal Interactions, 7:33, 2007.

[6] Y. Long, Z. Du, C. Chen, W. Wang, L. He, X. Mao, G. Xu, G. Zhao, X. Li, and W. Dong. Development and analysis of an electrically actuated lower extremity assistive exoskeleton. Journal of Bionic Engineering, 14(2):272–283, 2017.

[7] M. W. Payne, D. R. Williams, and G. Trudel. Space flight rehabilitation. American Journal of Physical Medicine Rehabilitation, 86:583–591, 7 2007.

[8] F. Sado, H. J. Yap, R. A. R. Ghazilla, and N. Ahmad. Design and control of a wearable lower-body exoskeleton for squatting and walking assistance in manual handling works. Mechatronics, 63:102272, 2019.

[9] van Dijk et al. Exobuddy-a non-anthropomorphic quasi-passive exoskeleton for load carrying assistance. In 2018 7th IEEE International Conference on Biomedical Robotics and Biomechatronics (Biorob), pages 336–341. IEEE, 2018.

[10] T. Wang, Y. Zhu, T. Zheng, D. Sui, S. Zhao, and J. Zhao. PALExo: A parallel actuated lower limb exoskeleton for high-load carrying. IEEE Access, 8:67250–67262, 2020.